Machine learning-based prediction of breast cancer growth rate *in-vivo*

Shristi Bhattarai[1*], Sergey Klimov[1*], Mohammed A Aleskandarany[2], Helen Burrell[3], Anthony Wormall[2], Andrew R Green[2], Padmashree Rida[1], Ian O Ellis[2], Remus M Osan[4], Emad A Rakha[2¥] and Ritu Aneja[1 ¥]

[1]Departments of Biology, Georgia State University, Atlanta, GA 30303; [2]Division of Cancer and Stem Cells, School of Medicine, University of Nottingham and Nottingham University Hospitals NHS Trust, City Hospital Campus, Nottingham, NG5 1PB, UK; [3]Department of Radiology, Nottingham University Hospitals NHS Trust, Nottingham City Hospital, Nottingham, NG5 1PB, UK; [4]Mathematics and Statistics, Georgia State University, Atlanta, GA 30303.

[¥]Correspondence:

Ritu Aneja, PhD

Department of Biology, Georgia State University, PSC 614

100 Piedmont Ave, Atlanta GA 30303

Office: 404-413-5417

Fax: 404-413-5301

Email: raneja@gsu.edu

Or

Emad A. Rakha, PhD

Division of Cancer and Stem Cells

School of Medicine, University of Nottingham City Hospital Campus

Hucknall Road

Nottingham

NG5 1PB, UK

Telephone: 01159691169 Ext: 56416

Fax: (+44) 01159627768

Email: emad.rakha@nottingham.ac.uk, emad.rakha@nuh.nhs.uk

*** equal contribution**

Keywords: Breast cancer, growth rate, predictors, *in-vivo*, mammograms

Disclaimers: The authors declare no conflict of interest

ABSTRACT

Background: Determining the rate of breast cancer (BC) growth *in-vivo*, which can predict prognosis, has remained elusive despite its relevance for treatment, screening recommendations and medicolegal practice. We developed a model that predicts the rate of *in-vivo* tumor growth using a unique study cohort of BC patients who had two serial mammograms wherein the tumor, visible in the diagnostic mammogram, was missed in the first screen.

Methods: A **S**erial **M**ammography-derived ***In-vi****vo* **G**r**o**wth **R**ate (*SM-INVIGOR*) index was developed using tumor volumes from two serial mammograms and time interval between measurements. We then developed a machine learning-based surrogate model called *Surr-INVIGOR* using routinely-assessed biomarkers to predict *in-vivo* rate of tumor growth and extend the utility of this approach to a larger patient population. *Surr-INVIGOR* was validated using an independent cohort.

Results: *SM-INVIGOR* stratified discovery cohort patients into fast- versus slow- growing tumor subgroups wherein patients with fast-growing tumors experienced poorer BC specific survival. Our clinically relevant *Surr*-INVIGOR stratified tumors in the discovery cohort and was concordant with *SM-INVIGOR*. In the validation cohort, *Surr-INVIGOR* uncovered significant survival differences between patients with fast- and slow-growing tumors.

Conclusion: Our *Surr-INVIGOR* model predicts *in-vivo* BC growth rate during the pre-diagnostic stage, and offers several useful applications.

BACKGROUND

Breast cancer (BC) is a heterogeneous disease with tumors exhibiting variable morphology, molecular profiles, behavior, and response to therapy. Mounting evidence demonstrates that BC shows variable rates of growth, which has important clinical and medicolegal implications (1-4). *In-vivo* growth rate is not only a quantifiable trait of the tumor but can also serve as a tool to plan and evaluate screening programs, clinical trials or epidemiologic studies. In addition, BC growth rate evaluated using tumor size from mammograms may predict tumor response to chemotherapy and may help in determining the likely time of tumor initiation and previous tumor size in medicolegal cases (5-7). BC growth rate is also associated with prognostic variables such as lymph node status, stage and vascular invasion (3, 4, 8); however, the prognostic and predictive value of BC growth rate has not been harnessed in routine practice due to the inherent difficulty in its assessment in the short intervals between diagnosis and treatment.

Although the growth rate of BC *in-vivo* is strictly regulated, it appears to be dependent on the balance between several variables including growth fraction (the tumor cells that are proliferating and leading directly to the addition of new tumor cells), the rate of tumor cell loss by apoptosis and/or necrosis, tumor cells' doubling-time/kinetics, and the surrounding microenvironment including angiogenesis, blood supply, and host immune response to the proliferating tumor cells (9-12). The complexity of the processes controlling BC growth and the interaction with the tumor microenvironment make assessment and prediction of BC growth rate a challenging task. Therefore, serial imaging of BC at different time points is considered as the best model available for assessing the *in-vivo* growth rate and for determining associations between potential intrinsic growth rate determinants and BC behavior, including response to therapy.

This study utilizes a discovery cohort comprising clinically and molecularly well-characterized data from BC patients who underwent serial mammography. It is a unique and rare cohort because the second mammogram illuminated that the tumor was indeed "missed" during the first mammogram. We find that this one-of-a-kind cohort can be interrogated to (a) identify predictors of BC *in-vivo* growth rate, (b) evaluate the impact of BC growth rate on disease outcome, and (c) develop a surrogate model that robustly predicts pre-diagnosis *in-vivo* growth rate for patients who would normally not have tumor volume data from two serial mammograms. In contrast to a matched first-presentation-only BC patients' cohort, BC growth rate in this study is determined by the changes in tumor volume between sequential mammograms, wherein the first mammogram "mistakenly" reported the case as normal/benign and the cancer was identified in the screening mammogram on a retrospective review subsequent to the second (diagnostic) mammogram (**Figure 1**).

METHODS

Study cohort: The study cohort comprised of 114 BC patients aged between 50-70 years who were presented at the Nottingham City Hospital from 1988 to 2008 with BC, and for whom review of the previous screening mammogram showed a previously undetected tumor at the same affected site. This may have been due to either a false-negative screening outcome, or due to minimal visible signs of malignancy on the previous mammogram. Mammographic abnormalities included measurable soft tissue abnormality (mass, distortion or asymmetry) on screening and diagnostic films. On retrospective review of the previous mammogram after the disease diagnosis, two radiologists (blinded to each other's observations) confirmed the "missed" cancer. We selected patients in whom a soft tissue abnormality was detected (upon retrospective review of prior screening mammograms) at the site of the subsequent cancer. Due to a misdiagnosed mammogram, this cohort uniquely comes with an earlier screening measurement with a visible tumor. Clinicopathological data including age, histological tumor type, primary tumor size, lymph node status, histological grade, Nottingham Prognostic Index

(NPI), vascular invasion and patients' outcome data were obtained. BC-specific survival (BCSS) was defined as the time interval (in months) between the primary surgeries and death from BC. The mean survival time of this cohort of patients was 120 months. Clinicopathological variables were available for 92 cases and the BCSS was available in 90 cases; thus, we restricted our study to these cases (**Figure 1A**).

Calculating tumor volumes and growth rates: The two measurements in the screening and diagnostic mammograms were assumed as tumor diameter and tumor height, which were then used to calculate tumor volumes at the time of screening and diagnosis. The greater mammogram dimension was assumed as height corresponding to the diameter of the semi-major axis, and the other dimension was regarded as diameter of the semi-minor axis. For tumor volume calculation, we considered the aforementioned dimensions as volume inputs for a cylinder, sphere, and an oblate spheroid (13). For tumor growth rates, we tested exponential growth (14, 15), the Gompertz model (16), and power law growth with the exponent set to both the classic value of 2/3 (17, 18) and 1/2 (19) as shown in **Table S1**. For all models, the initial volume for the growth rate was determined using the screening mammogram and the final volume was determined from the diagnostic mammogram, with the time variable denoted by the days between the two mammograms.

Selecting optimal tumor volume, growth rate combination and development of SM-INVIGOR: Multiple tumor volume/three-dimensional shape assumptions and growth rate functions used in previous studies (19), were tested to find the optimal combination that was prognostic. Growth rate indices that combined tumor volume (calculated assuming the tumor to be a sphere, cylinder, or spheroid) and individual growth functions (calculated assuming exponential growth, two sets of the Power Law function (α =1/2 or 2/3), or Gompertz growth), were compared on the basis of their prognostic ability. Growth rates were used either as a continuous variable or through a fast/slow growth cutoff determined through optimizing the log-rank statistic (20, 21). Both forms of all growth rates were analyzed univariately in a Cox proportional hazard regression model using 10-year breast cancer specific survival (BCSS), and corresponding model fits were ranked with the Akaike Information Criterion (AIC) (22). The best-fitting growth rate index was chosen via the lowest relative AIC and was used in subsequent analyses. Data related to changes in volume of the lesion between the time of screening and at diagnosis, as well as the time between screening and diagnosis, were used to estimate the **S**erial **M**ammography-derived ***In-vi****vo* **Gro**wth **R**ate (*SM-INVIGOR*) (**Figure 1B).** To control for common clinicopathological confounders, the growth rate model was also analyzed with multivariate Cox regression alongside grade, age, and estrogen receptor (ER) status. In addition, the tumor volumes at the screening and diagnostic time-points were tested prognostically to evaluate the prognostic significance of the change in tumor volume versus that of the screen- or diagnostic mammogram-calculated volume individually (**Figure 1C**).

Assessing and scoring immunohistochemical staining: For each patient, a representative formalin-fixed paraffin wax-embedded (FFPE) tumor block of the resected tumor was obtained from the Nottingham breast tumor bank (**Figure 1D**). Full-face sections 4 μm thick from the representative FFPE tumor blocks were prepared onto Xtra® Surgipath glass slides and were used for immunohistochemical (IHC) assessment of the following markers: estrogen receptor (ER), progesterone receptor (PR), HER2 (human epidermal growth factor receptor 2), the proliferation markers Ki67 and MCM2 (Minichromosome Maintenance 2), the basal markers CK5/6 (cytokeratin 5/6) and EGFR epidermal growth factor receptor), the apoptosis markers BCL2 and cleaved caspase-3. IHC was performed on tissue sections using Novolink™ Max Polymer Detection System. (Leica, Newcastle, UK). Briefly, heat-assisted retrieval of antigen epitopes was performed in citrate buffer (pH 6) using a microwave for 20 minutes, followed by immediate cooling. The slides were rinsed with Tris-Buffered Saline (TBS, pH 7.6). The primary antibodies as summarized in Table S2 were applied for 30 minutes at room temperature except for cleaved caspase-3 staining. For cleaved caspase-3 a pre-fabricated detection kit (*SignalStain® Cleaved Caspase-3 (Asp175) IHC Detection Kit #8120, Cell Signaling Technology)* was used following manufacturer's instructions. Other markers were stained using our protocols as previously published (23, 24).

Appropriate positive and negative controls were used for each marker and included in each staining run. Only the invasive tumor cells were scored independently by two observers (SB and MA) blinded to each other's scores and clinicopathological data. Cases with discordant results were further reviewed by both observers to achieve scoring consensus. For each marker, the percent and intensity of staining were assessed, and H-scores were generated. For ER, PR, and HER2, cut-offs according to published guidelines were used (25, 26). Ki67, and cleaved caspase-3 were assessed and scored as previously described (23, 24). BC molecular subtypes were defined based on their IHC expression profile into: a) luminal (ER+ and/or PR+ /HER2-), b) HER2+ (HER2-positive), c) Triple negative (TN; ER-, PR-, HER2-) and d) Basal-like Breast cancer (BLBC: TN+ CK5/6+) (24). A total of 92 cases were informative for IHC biomarkers and these comprised the study cohort in the subsequent analyses including molecular markers (**Figure 1E**).

***Development of the machine learning-based surrogate model (Surr-INVIGOR)*:** The above mentioned clinical and molecular variables, and immunohistochemical biomarkers (**Table S3**) were evaluated using machine learning algorithms to identify an optimal feature set that could serve as a surrogate model for *SM-INVIGOR* to predict fast or slow *in-vivo* growth rate for cases where only a single (diagnostic) mammogram is available (**Figure 1F/G/H**). The significance of mean differences for all potential surrogate variables, between fast- and slow-growing tumors, was first calculated using a 2-tailed t-test; this was followed by a ranking of the variables based upon their discriminating capacity. Multiple classification algorithms (support vector machines,, naïve Bayes, decision trees, discriminant analysis, ensemble), with optimized hyperparameters (27, 28) were then tested. The machine learning algorithm and feature set that resulted in the maximum 5-fold cross-validated accuracy (mean of 100 iterations) was chosen. For each trained machine learning model (combination of biomarkers), hyperparameters were fit through Bayesian optimization (27, 28) over 180 iterations (**Table S4**). Furthermore, a combination of variables was used, in an optimized regression model, to identify if the continuous growth rate value for each patient could be determined. Finally, the outputs from the machine learning-based approach were compared to the regression-based models which did not yield good R^2 values owing to small sample size.

Validation of Surr-INVIGOR: The prognostic performance of this surrogate model (*Surr-INVIGOR*) was tested in an independent, well-characterized large validation cohort of 1241 BC patients using Kaplan-Meier survival analysis (**Figure 1I/J**). Multivariate Cox regression was used to control for confounding effects of common clinicopathological variables.

Statistical analysis: All statistical analyses were carried out with SAS 9.4 ® software and MATLAB Version 9.2. Clinicopathological proportion differences between growth groups were determined using the $\chi 2$ test. Continuous clinicopathological variable differences were evaluated via a 2-tailed t-test. Prognostic time to event analysis was performed using Kaplan-Meier and Cox Proportional Hazard regression, wherein a death due to BC was considered as an event and every other outcome was censored. For all analyses, $p<0.05$ was considered significant.

RESULTS

Clinicopathological and molecular features of cases in the study cohort

Most patients in the study cohort showed features associated with good prognosis including lower grade and negative (65%) or early positive (pN1; 26%) lymph nodes. Age at the time of diagnosis ranged from 50 to 73 years (mean=60.3 years, median=61.0 years). There was a predominance of the luminal A subtype with 85% positive for ER while HER2 overexpression was identified in only 6% of the patients. Ki67 staining ranged from 0 to 96%, with a mean expression of 19% (**Table 1**). Moreover, there was a significant correlation between the histological tumor size and the mammogram tumor size at time of diagnosis (Pearson's correlation=0.58870; $p<0.0001$).

Development of SM-INVIGOR, a significant predictor of breast cancer-specific survival

Since fast *in-vivo* growth prior to diagnosis is a sign of aggressive disease and could lead to poor outcomes, we reasoned that the growth rate model of choice would be the one that is most prognostic. Thus, we evaluated various combinations of growth rate functions and assumptions regarding the tumor's three-dimensional shape. The best fitting model of tumor volume and growth rate was obtained using the assumption that the study cohort comprises spherical tumors growing at a power law ($\alpha=0.5$) rate; this growth rate function (*SM-INVIGOR)* stratified the tumors into slow-growing and fast-growing subgroups and produced a minimum cross validated AIC of 152.621 (**Table S5**). Using these assumptions, tumor volumes at the time of screening ranged from 53-56,115 mm^3 (mean of 2,742 ± 7,619 mm^3). This contrasted with tumor volumes at diagnosis, which ranged from 61 to 61,562 mm^3 (mean=5,573 ± 8,768 mm^3). The mean time difference between date of first screening and that of second diagnostic screening was 18 months, (range 4-37 months, median=17.5 months). Tumor growth rate differed considerably from patient to patient, ranging from 0 to 0.53 mm^3/day (mean=0.08 ± 0.13 mm^3).

SM-INVIGOR used a cutoff of 0.045 mm^3/day to stratify tumors into slow-growing (n=53) and fast-growing (n=37) subgroups. Faster *SM-INVIGOR* significantly associated with clinicopathological factors normally associated with poorer prognoses, such as larger histological tumor size ($p=0.0023$), high grade (Grade 3) ($p=0.0186$), more mitotic divisions ($p=0.0134$), apparent vascular invasion ($p=0.0139$), and a poor Nottingham Prognostic Index ($p=0.011$) (**Figure 2A).** *SM-INVIGOR* varied significantly between BC molecular subtypes with the highest rate observed in triple-negative BC (TNBC) compared to other subtypes ($p<0.05$). Among the proliferation/apoptosis-related biomarkers that were immunohistochemically assessed (**Table S3**), only Ki67 showed a significant mean difference ($p=0.0003$) between the fast- (24%) versus slow- growing (11%) tumor subgroups. Furthermore, patients with higher tumor growth rate showed significantly poorer survival (BCSS=71.7%) relative to the slow-growing tumors (BCSS=91.9%) as shown in Kaplan Meier's survival graph (**Figure 2B).** *SM-INVIGOR* retained prognostic significance ($p=0.0299$, high growth rate HR=4.605) upon controlling for common clinicopathological variables including grade, age and ER status. In fact, *SM-INVIGOR* was the only variable significantly associated with BCSS in our multivariable analysis **(Figure 2C)**.

Development of a clinically-relevant surrogate model (Surr-INVIGOR) for in-vivo growth rate prediction

Unlike the patients in our unique discovery cohort, most begin therapy at an initial cancer diagnosis, and are therefore unlikely to have two serial mammograms with two tumor volume measurements. Because of this difference, *SM-INVIGOR* is limited in its utility to derive in-vivo tumor growth rate for most BC patients in routine clinical practice. Therefore, to extend the benefits of having growth rate data (or estimates) to a much larger group of patients lacking a second mammogram, we developed a machine learning-based surrogate growth rate model for *SM-INVIGOR* and called it *Surr-INVIGOR* (described in Suppl. data). *Surr-INVIGOR* non-linearly combines multiple clinicopathological variables and immunohistochemical biomarkers to predict *in-vivo* growth rate. First, we evaluated the ability of individual clinicopathological variables to serve as potential surrogate features and discriminate between the fast- and slow- growing tumor subgroups of our study cohort (p-values for mean difference between the subgroups is shown in **Table S4**. Ki67 (p=0.000265), mitotic score (MI; p=0.002479), tumor size (p=0.003619), NPI (p=0.004163), and grade (p=0.021128) differed significantly between the fast- and slow- growing tumors. The seven variables (Ki67, Mitotic score, tumor size, NPI, Grade, Stage and Tumor size) with p value <0.2 were then tested in multiple machine learning-based classification algorithms via sequential selection (**Figure S1**). The maximized cross-validated accuracy, which indicates the optimal *Surr-INVIGOR* model, was obtained when three features (Ki67, MI, and histological tumor size) were used in a K-nearest neighbor algorithm or KNN (accuracy or concordance with the classification yielded by *SM-INVIGOR*=0.706). The Ensemble also yielded a 70% accurate classifier but required 4 additional features; the more parsimonious KNN was thus selected for use in *Surr-INVIGOR*. Fitting an optimal regression model to predict the growth rate continuously resulted in a poor R^2, peaking at 0.22, as shown in **Figure S2,** perhaps owing to the small sample size. Thus, our machine learning-based *Surr-INVIGOR* model was a clinically-relevant, superior choice compared to regression-based models.

Validation of Surr-INVIGOR in an independent BC case series demonstrates its robust prognostic value

We then evaluated the prognostic ability of *Surr-INVIGOR* in an independent BC case series (n=1241) from Nottingham University Hospital, UK. Patient age at the time of diagnosis ranged from 21-71 years (mean=53.6 years, median=54 years). Most patients showed features associated with good prognosis including negative lymphovascular invasion (55.3%), and negative (61%) or showed 1-3 positive (30%) lymph nodes. Patient follow up time ranged from 1 to 120 months (mean=100.237, median=120 The clinicopathological features of patients are summarized in Table 1.

The clinicopathological variables that discriminated between slow- and fast-growing tumors are depicted in **Figure 2D.** Applying the previously-trained *Surr-INVIGOR* model, using the same input parameters on this naïve validation cohort resulted in significant BCSS stratification. Patients in the fast growth rate group (n=922, BCSS=72.9%) had a significantly lower survival than patients in the slow growth rate group (n=269, BCSS=92.3%) **Figure 2E.** After accounting for potential clinicopathological cofounders, *Surr-INVIGOR* retained prognostic significance (HR=1.758, p=0.0361) alongside grade as shown in **Figure 2F.**

Surr-INVIGOR can be used to determine tumor age at diagnosis in a subset of breast tumors

Using the different growth rate groups, we can estimate tumor age and the time of inception of a subset of tumors. Assuming the highest (bounded) power law (α=0.5) growth rate (0.04593 mm^3/day) for the slow-growing subgroup, we can estimate the date after which the tumor was definitely present within the patients in the slow-growing tumor subgroup. Using these assumptions, we determined that the average tumor age at diagnosis of slow-growing tumors was 4.7 years (**Figure S3)**. Using this methodology, it may be possible to determine whether a patient possessing a slow-growing tumor undetected at earlier screenings, had received a true-negative or false-negative (i.e., tumor was missed) screening result.

DISCUSSION

Although several studies have investigated variables associated with pre-diagnosis *in-vivo* BC growth rate, only clinicopathological variables and a few molecular biomarkers have been studied in this context and the available tumor dimensions were limited due to the measurement of the tumor's long-axis only (2, 5, 29, 30). This study utilized a unique cohort of cases with tumor volume measurements (derived using tumor diameter and height data) available from a pair of serial mammograms to derive their *in-vivo* growth rates (*SM-INVIGOR*). We explored the potential association of a larger number of molecular biomarkers with their *in-vivo* BC growth rate, reaffirmed that fast tumor growth rate has a profound impact on prognosis, developed and validated a surrogate model (*Surr-INVIGOR*) that can predict a gross scale (fast versus slow) *in-vivo* growth rate accurately in routine practice, and its medicolegal consequences.

The success of breast screening lies in the timely detection of cancer on mammography. False negative mammography is among the principal reasons for delayed diagnosis of BC(31-34). Even though some authors quote high sensitivity (>90%) for diagnostic mammography, such results are not universal (35). Among many factors, age appears to be one of the important factors underlying false negative reporting because the high radiographic density of breast in young women makes detection difficult (6). Mammograms are generally capable of detecting tumors as small as 2 mm in diameter, which equates to a tumor of approximately 10^7 cells and about 23 tumor doublings (36). In our study cohort, however, patients with tumors ranging from 4-55 mm received false-negative diagnoses in their screening mammograms, showing the imperfection associated with this technology and inherent human limitations associated with reading radiology films. Whether the spread of a tumor is due to delays in diagnosis and initiation of treatment, or due to the inherently more aggressive nature of the tumor cells themselves (i.e., higher *in-vivo* tumor growth rate) is another highly controversial matter. Natural fears that the delay in diagnosis has reduced their chances of survival or of avoiding the life-sapping effects of chemotherapy, or the feeling that cosmetic outcomes which would have been better had the tumor been detected earlier, are frequent causes of patients seeking legal redress. The importance of breast imaging in BC diagnosis and the use of mammography in screening has thus pushed breast radiologists into the frontline for medicolegal actions (37). Cancers missed at screening but followed by a positive diagnostic mammogram are not common yet false negative mammography is among the principal reasons for delayed diagnosis of BC (31-34). Only few population-screening programs have reported data on this group of cancers, which makes our study cohort uniquely valuable. This cohort allowed us to develop a model to predict pre-diagnostic *in-vivo* tumor growth rate and provide insights into the potential prognostic consequences of delays in BC diagnosis.

Our study has yielded several key insights into features and the prognostic significance of the rate of tumor growth in its early stages. In our study, we found that *SM-INVIGOR* varies considerably and is consistent with findings by Weedon-Fekjaer and colleagues (5) who reported that the time BC takes to grow from 10 mm to 20 mm in diameter varied from less than 1.2 months to more than 6.3 years. Our current study also reinforced previous findings that higher grade and larger tumors with high proliferative activity are likely to have faster *SM-INVIGOR* and that faster pre-diagnosis growth rate predicted shorter survival (2, 5, 29, 30, 38, 39). We also found that the status of lymphovascular invasion (LVI) correlated with growth rate; with highly proliferative and fast-growing tumors more likely to develop when there is increased provision of nutrients to the tumor cells from the leaky invaded blood vessels. Our results indicated that increasing *SM-INVIGOR* increases the risk of mortality of the disease. However, *SM-INVIGOR* cannot be included as a prognostic variable in routine clinical practice because of difficulty in evaluating it in the short interval between diagnosis and treatment.

Therefore, we developed *Surr-INVIGOR* to predict the pre-diagnosis *in-vivo* BC growth rate after testing multiple clinicopathological and molecular variables (individually and in combination) using diverse machine learning algorithms. The optimal algorithm, a KNN which used Ki67, MI, and size, stratified both the study and validation cohorts into two subgroups with very distinct outcomes. *Surr-INVIGOR* further allowed routine clinical parameters to be used in patients with slow-growing tumors to determine tumor size at various time-points before the diagnosis of the tumor. For fast-growing tumors, immediate surgery is often recommended, as delays may result in upgrading of clinical T stage. *Surr-INVIGOR* may thus have a potential use in medicolegal cases, and may be used to guide screening and perhaps even follow-up intervals in selected groups of BC patients.

Consistent with previous studies (40, 41), results from our validation cohort showed a significant correlation between BC molecular subtypes and pre-diagnosis tumor growth rate wherein a higher growth rate was observed in triple negative/basal-like BC patients. Previous studies have indicated that faster growing tumors lead to poorer survival (42-45). Our results compellingly demonstrated that high pre-diagnosis *in-vivo* BC growth rate increases the risk of mortality from the disease regardless of potential clinicopathological cofounders. Some previous studies did not find such statistically significant associations (3, 4), which might be because in those studies, the tumor volume was calculated using only one dimension-a method that can introduce considerable inaccuracy into growth rate calculations. In the current study, we utilized a combination of power law growth rate and spherical volume-both of which were significant in a previous study using 2-dimensional breast mammogram data (19), and showed the most significant prognostic relevance in our data.

Review of previous mammography is carried out as a routine practice at Nottingham Hospital, and cases that show an abnormality at the same site as the diagnosed tumors are considered as cancers potentially missed in the prior screening. Some of these tumors are only detectable in retrospect with knowledge of the diagnostic mammograms, and if all such subtle areas were recalled for further assessment, this would likely increase the false positive rate beyond what is regarded as acceptable in the NHS breast screening program. The impact of such delay in the diagnosis on the presentation and outcome of these tumors compared to matched population of women who presented for the first time as symptomatic or with screen-detected BC remains to be defined. Most tumors included in our study (similar to other studies looking at screen-detected tumors) by their very nature, were small, slow-growing luminal tumors, and infrequently expressed basal markers or HER2 with similar nodal status (30). This can be explained by the unique nature of these slow growing early-stage tumors in this study. By contrast, aggressive tumors are likely to present without prior mammographic abnormality (46). In line with these results, Kalager et al. (47) have reported that BCs presenting as interval cancers were slightly larger than symptomatic BC but there was no difference between the two groups regarding lymph node status or patient outcome. Moreover, our results indicated that the impact of *SM-INVIGOR* on disease stage and development of LVI is limited. However, the present study holds a few limitations: due to the unique nature of the study cohort and the lack of similar missed cancer cohorts, the *SM-INVIGOR* growth index could not be readily validated. Additionally, this is a retrospective, single center study and adjuvant treatment regimens were not factored in our analyses. Validation of the model in diverse cohorts is necessary before it can be applied for the prediction of in-vivo growth rate and determination of the likely tumor initiation date and previous tumor size in clinico-legal cases. If validated in further studies, the model developed herein could potentially guide treatment selection as it prognostically distinguishes fast-growing tumors from slow-growing ones. For example, for fast growing tumors, immediate treatment in the form of primary systemic therapy (rather than surgery) may be required. Moreover, HER2 is known to be related to rapid growth of tumors and might be a good marker to add to the *Surr-INVIGOR*, however our study cohort was overwhelmingly HER2 negative and thus it's impact within a prognostic model could not be properly measured. Further analysis may be required in a diverse cohort.

In conclusion, this study has demonstrated that multiple factors control BC growth; when considered together Ki67, Mitotic Index, and tumor size produce a robust prediction model of pre-diagnostic growth rate and can be used to classify BCs as slow- or fast- growing. The impact of missing subtle cancers in screening mammography seems to depend on whether the tumor was slow- or fast- growing prior to diagnosis, as fast-growing tumors were associated with poorer outcomes and perhaps reflected more aggressive tumor biology. Independent validation of these findings in multiple and more diverse cohorts is warranted.

ADDITIONAL INFORMATION

Ethics approval and consent to participate: This study was approved by the Nottingham Research Ethics Committee 2 under the title 'Development of a molecular genetic classification of breast cancer'. All samples from Nottingham used in this study were pseudo-anonymized and collected prior to 2006 and therefore under the Human Tissue Act (UK, 2006), informed patient consent was not needed. Release of data was also pseudo-anonymized as per Human Tissue Act regulations.

We can declare that this study is complying with Helsinki declaration.

Consent for publication: N/A

Availability of data and materials: All the data and results generated during the study can be provided upon journal request.

Conflict of Interest: “The authors declare no conflict of interest”.

Funding: The study was supported by grants to RA from the National Cancer Institute at the National Institute of Health (U01 CA179671 and R01 CA169127).

Authorship:

1. SB: Study design, experiments, analysis and writing manuscript
2. SK: Statistical analysis, machine learning model, and writing manuscript
3. MA: Identifying cases, experiments and editing manuscript
4. HB: Identifying cases
5. AW: Identifying cases and study design
6. AG: Identifying cases and study design
7. PR: Discussion and editing manuscript
8. IE: Study support
9. RO: Help with data analysis
10. ER: Study design, manuscript editing, financial support and overall study supervision
11. RA: Study design, manuscript editing, financial support and overall study supervision

Acknowledgements: We would like to sincerely thank Dr. Emiel A.M Janssen for discussions and help with editing of the manuscript. We also thank the Nottingham Health Science Biobank for providing tissue samples.

REFERENCES

1. Brekelmans CT, van Gorp JM, Peeters PH, Collette HJ. Histopathology and growth rate of interval breast carcinoma. Characterization of different subgroups. Cancer. 1996;78(6):1220-8.
2. Hart D, Shochat E, Agur Z. The growth law of primary breast cancer as inferred from mammography screening trials data. British journal of cancer. 1998;78(3):382-7.
3. Tubiana M, Pejovic MH, Koscielny S, Chavaudra N, Malaise E. Growth rate, kinetics of tumor cell proliferation and long-term outcome in human breast cancer. International journal of cancer. 1989;44(1):17-22.
4. Yoo TK, Min JW, Kim MK, Lee E, Kim J, Lee HB, et al. In Vivo Tumor Growth Rate Measured by US in Preoperative Period and Long Term Disease Outcome in Breast Cancer Patients. PloS one. 2015;10(12):e0144144.
5. Weedon-Fekjaer H, Lindqvist BH, Vatten LJ, Aalen OO, Tretli S. Breast cancer tumor growth estimated through mammography screening data. Breast cancer research : BCR. 2008;10(3):R41.
6. Andrews BT, Bates T. Delay in the diagnosis of breast cancer: medico-legal implications. Breast (Edinburgh, Scotland). 2000;9(4):223-37.
7. Berry DA, Cronin KA, Plevritis SK, Fryback DG, Clarke L, Zelen M, et al. Effect of screening and adjuvant therapy on mortality from breast cancer. The New England journal of medicine. 2005;353(17):1784-92.

8. Galante E, Gallus G, Guzzon A, Bono A, Bandieramonte G, Di Pietro S. Growth rate of primary breast cancer and prognosis: observations on a 3- to 7-year follow-up in 180 breast cancers. British journal of cancer. 1986;54(5):833-6.
9. Arnerlov C, Emdin SO, Lundgren B, Roos G, Soderstrom J, Bjersing L, et al. Breast carcinoma growth rate described by mammographic doubling time and S-phase fraction. Correlations to clinical and histopathologic factors in a screened population. Cancer. 1992;70(7):1928-34.
10. Boyd NF, Meakin JW, Hayward JL, Brown TC. Clinical estimation of the growth rate of breast cancer. Cancer. 1981;48(4):1037-42.
11. Locopo N, Fanelli M, Gasparini G. Clinical significance of angiogenic factors in breast cancer. Breast cancer research and treatment. 1998;52(1-3):159-73.
12. Casey T, Bond J, Tighe S, Hunter T, Lintault L, Patel O, et al. Molecular signatures suggest a major role for stromal cells in development of invasive breast cancer. Breast cancer research and treatment. 2009;114(1):47-62.
13. Heuser L, Spratt JS, Polk HC. Growth rates of primary breast cancers. Cancer. 1979;43(5):1888-94.
14. Collins VP. Observation on growth rates of human tumors. Am J Roentgenol. 1956;76:988-1000.
15. Shackney SE. A computer model for tumor growth and chemotherapy, and its application to L1210 leukemia treated with cytosine arabinoside (NSC-63878). Cancer chemotherapy reports Part 1. 1970;54(6):399-429.
16. Gompertz B. On the nature of the function expressive of the law of human mortality, and on a new mode of determining the value of life contingencies. Philosophical transactions of the Royal Society of London. 1825;115:513-83.
17. Mandonnet E, Delattre JY, Tanguy ML, Swanson KR, Carpentier AF, Duffau H, et al. Continuous growth of mean tumor diameter in a subset of grade II gliomas. Annals of neurology. 2003;53(4):524-8.
18. Mayneord WV. On a law of growth of Jensen's rat sarcoma. The American Journal of Cancer. 1932;16(4):841-6.
19. Talkington A, Durrett R. Estimating tumor growth rates in vivo. Bulletin of mathematical biology. 2015;77(10):1934-54.
20. Contal C, O'Quigley J. An application of changepoint methods in studying the effect of age on survival in breast cancer. Computational statistics & data analysis. 1999;30(3):253-70.
21. Meyers JP, Mandrekar JN. Cutpoint Determination Methods in Survival Analysis using SAS®: Updated% FINDCUT macro.
22. Akaike H. A new look at the statistical model identification. IEEE transactions on automatic control. 1974;19(6):716-23.
23. Aleskandarany MA, Green AR, Benhasouna AA, Barros FF, Neal K, Reis-Filho JS, et al. Prognostic value of proliferation assay in the luminal, HER2-positive, and triple-negative biologic classes of breast cancer. Breast cancer research : BCR. 2012;14(1):R3.
24. Rakha EA, Elsheikh SE, Aleskandarany MA, Habashi HO, Green AR, Powe DG, et al. Triple-negative breast cancer: distinguishing between basal and nonbasal subtypes. Clinical cancer research : an official journal of the American Association for Cancer Research. 2009;15(7):2302-10.
25. Wolff AC, Hammond ME, Hicks DG, Dowsett M, McShane LM, Allison KH, et al. Recommendations for human epidermal growth factor receptor 2 testing in breast cancer: American Society of Clinical Oncology/College of American Pathologists clinical practice guideline update. J Clin Oncol. 2013;31(31):3997-4013.
26. Hammond ME, Hayes DF, Wolff AC, Mangu PB, Temin S. American society of clinical oncology/college of american pathologists guideline recommendations for immunohistochemical

testing of estrogen and progesterone receptors in breast cancer. Journal of oncology practice / American Society of Clinical Oncology. 2010;6(4):195-7.
27. Bull AD. Convergence rates of efficient global optimization algorithms. Journal of Machine Learning Research. 2011;12(Oct):2879-904.
28. Gelbart MA, Snoek J, Adams RP. Bayesian optimization with unknown constraints. arXiv preprint arXiv:14035607. 2014.
29. Peer PG, van Dijck JA, Hendriks JH, Holland R, Verbeek AL. Age-dependent growth rate of primary breast cancer. Cancer. 1993;71(11):3547-51.
30. von Fournier D, Weber E, Hoeffken W, Bauer M, Kubli F, Barth V. Growth rate of 147 mammary carcinomas. Cancer. 1980;45(8):2198-207.
31. Kern KA. Causes of breast cancer malpractice litigation. A 20-year civil court review. Archives of surgery (Chicago, Ill : 1960). 1992;127(5):542-6; discussion 6-7.
32. Lannin DR, Harris RP, Swanson FH, Edwards MS, Swanson MS, Pories WJ. Difficulties in diagnosis of carcinoma of the breast in patients less than fifty years of age. Surgery, gynecology & obstetrics. 1993;177(5):457-62.
33. Mann BD, Giuliano AE, Bassett LW, Barber MS, Hallauer W, Morton DL. Delayed diagnosis of breast cancer as a result of normal mammograms. Archives of surgery (Chicago, Ill : 1960). 1983;118(1):23-4.
34. Mitnick JS, Vazquez MF, Plesser KP, Roses DF. Breast cancer malpractice litigation in New York State. Radiology. 1993;189(3):673-6.
35. Walker QJ, Langlands AO. The misuse of mammography in the management of breast cancer. The Medical journal of Australia. 1986;145(5):185-7.
36. Plotkin D, Blankenberg F. Breast cancer--biology and malpractice. American journal of clinical oncology. 1991;14(3):254-66.
37. Bishop HM. Medico-legal aspects of delay in breast cancer diagnosis: the surgeon's perspective. Breast Cancer Research. 2006;8(1):P23.
38. Pinder SE, Wencyk P, Sibbering DM, Bell JA, Elston CW, Nicholson R, et al. Assessment of the new proliferation marker MIB1 in breast carcinoma using image analysis: associations with other prognostic factors and survival. British journal of cancer. 1995;71(1):146-9.
39. Urruticoechea A, Smith IE, Dowsett M. Proliferation marker Ki-67 in early breast cancer. J Clin Oncol. 2005;23(28):7212-20.
40. Seewaldt VL, Scott V. Images in clinical medicine. Rapid progression of basal-type breast cancer. The New England journal of medicine. 2007;356(13):e12.
41. Ryu EB, Chang JM, Seo M, Kim SA, Lim JH, Moon WK. Tumour volume doubling time of molecular breast cancer subtypes assessed by serial breast ultrasound. European radiology. 2014;24(9):2227-35.
42. Freimanis RI, Yacobozzi M. Breast cancer screening. North Carolina medical journal. 2014;75(2):117-20.
43. Heuser LS, Spratt JS, Kuhns JG, Chang AF, Polk HC, Jr., Buchanan JB. The association of pathologic and mammographic characteristics of primary human breast cancers with "slow" and "fast" growth rates and with axillary lymph node metastases. Cancer. 1984;53(1):96-8.
44. Olsson A, Borgquist S, Butt S, Zackrisson S, Landberg G, Manjer J. Tumour-related factors and prognosis in breast cancer detected by screening. The British journal of surgery. 2012;99(1):78-87.
45. Spratt JS, Spratt SW. Medical and legal implications of screening and follow-up procedures for breast cancer. Cancer. 1990;66(6 Suppl):1351-62.
46. Raja MA, Hubbard A, Salman AR. Interval breast cancer: is it a different type of breast cancer? Breast. 2001;10(2):100-8.

47. Kalager M, Tamimi RM, Bretthauer M, Adami HO. Prognosis in women with interval breast cancer: population based observational cohort study. Bmj. 2012;345:e7536.

Figure and Table Legends:

Figure 1: Schematic depicting sequences of steps in our study leading to the calculation of *SM-INVIGOR* and the development of *Surr-INVIGOR* that predicts *in-vivo* tumor growth rate in BC: Briefly, tumor volumes from two serial mammograms and the time interval between measurements in a unique dataset of 92 patients (**A**), were used to develop a growth rate index *SM-INVIGOR* (**B**), The growth index significantly predicts BCSS and classifies tumors as slow- or fast-growing (**C**). When the tumors were resected after final diagnosis (**D**), tumor sections were immunohistochemically stained for a panel of BC biomarkers (**E**). A machine learning algorithm was used to develop a surrogate model (termed *Surr-INVIGOR*) for *SM-INVIGOR* that uses routinely assessed BC clinical biomarkers like Ki67, Mitotic Index and Histological size. The multivariable model non-linearly combines multiple clinicopathological variables and immunohistochemical biomarkers to predict the tumor's *in-vivo* growth rate prior to diagnosis (**F,G**). Using the same growth rate threshold as *SM-INVIGOR*, the *Surr-INVIGOR* model was able to prognostically stratify patients in study cohort (**H**). Finally, *Surr-INVIGOR* was validated using an independent BC validation cohort of 1241 patients and was found to be strongly prognostic in the validation cohort (**I,J**).

Figure 2: Prognostic significance of *SM-INVIGOR*. (A) Univariate associations between clinicopathological parameters and *SM-INVIGOR*. **(B)** Kaplan-Meier survival curve for study cohort patients stratified into high and low growth rate groups by SM-INVIGOR. **(C)** Multivariable analysis of the association between clinicopathological variables and outcome {breast cancer specific survival (BCCS)} in study cohort. **(D)**Univariate association between clinicopathological parameters and *Surr-INVIGOR* in validation cohort. **(E)** Kaplan-Meier survival curve for patients stratified into high and low growth rate subgroups by *Surr-INVIGOR* in validation cohort. **(F)** Multivariable analysis of the association between clinicopathological variables and BCSS in validation cohort.

Table 1: Clinicopathological characteristics of cases in the study cohort and validation cohort.

Tumor missed in screening mammogram
Tumor detected in diagnostic mammogram
Tumor Genesis
Time
Patient Outcomes
Initial Volume
Final Volume
Pre-diagnostic Period of Tumor Growth in vivo
Study Cohort
Validation Cohort
A
STUDY COHORT of patients with tumor volume data from 2 serial mammograms (n=92)
B
Tumor Growth Rate Calculation
C
Developed SM-INVIGOR which stratifies tumors in study cohort
Breast Cancer Specific Survival
Low Growth Rate
p<0.05
High Growth Rate
Survival Time (Years)
SM-INVIGOR's clinical utility is limited since most patients lack tumor volume data from 2 serial mammograms
D
Tumor Resection
E
Study cohort sections stained for routinely assessed BC biomarkers
F
ML and feature selection approach used to create model to predict SM growth groups
G
Surr-INVIGOR includes Ki67, MI & tumor size
Ki67
Mitotic Index
Histological Size
H
Surr-INVIGOR stratifies tumors in study cohort
I
Surr-INVIGOR tested on large validation cohort (n=1241) of BC patients
J
Surr-INVIGOR stratifies tumors in VC

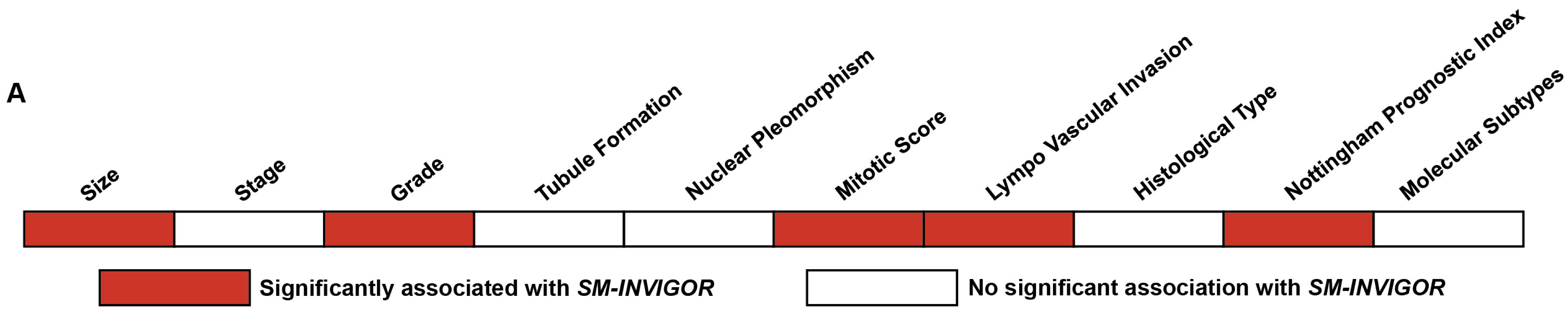

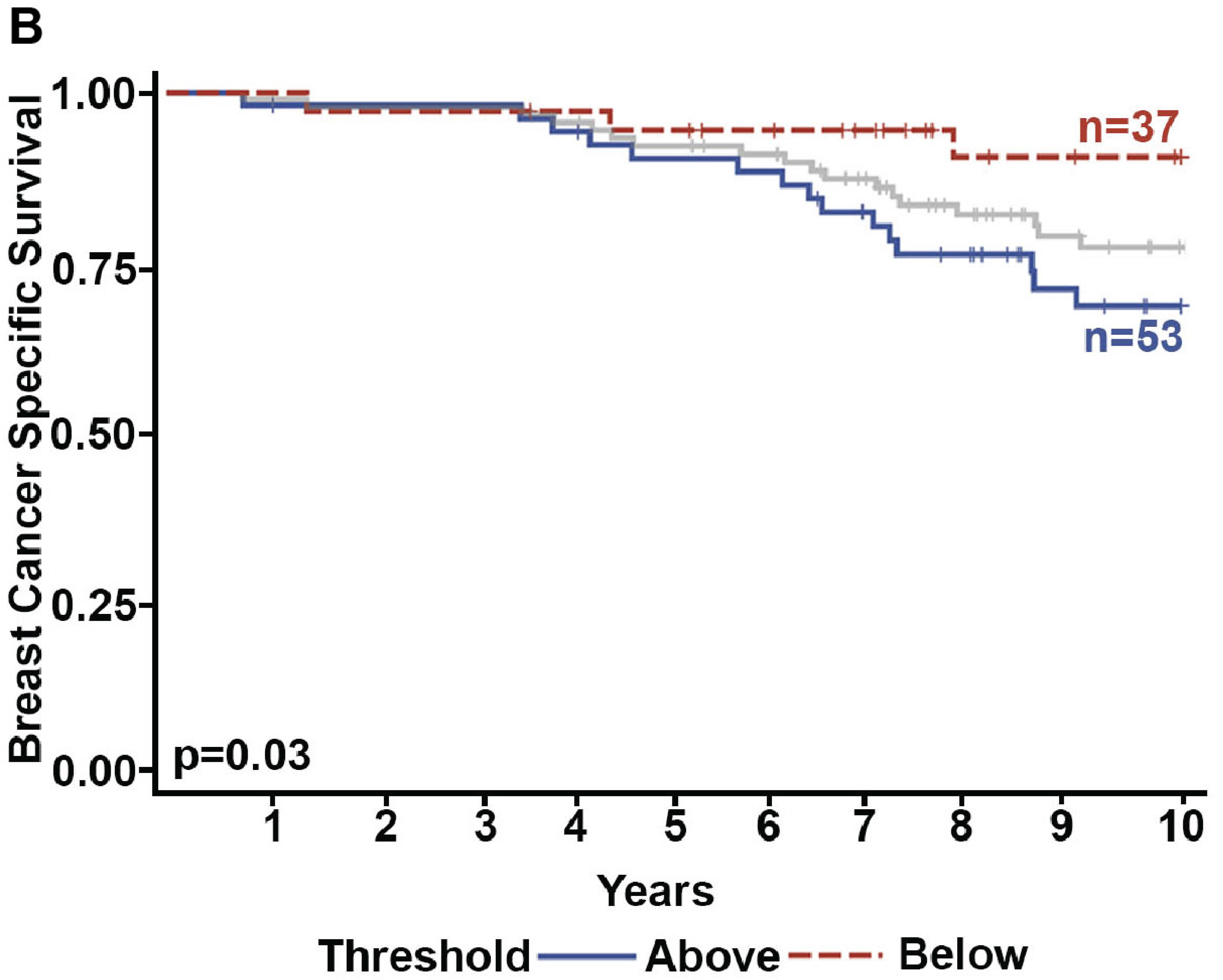

C

Multivariate analysis of the association between clinicopathological variables and patient's outcome in the study cohort			
		Hazard Ratio (95% CI)	p-value
Overall Survival			
Age	≤65 vs >65	0.989 (0.912-1.072)	0.78
ER	Neg	0.836 (0.229-2.98)	0.77
Grade	3	3.684 (0.043-30.623)	0.22
Grade	2	4.877 (0.615-38.702)	0.13
SM-INVIGOR	Above	3.623 (1.014-12.941)	0.04

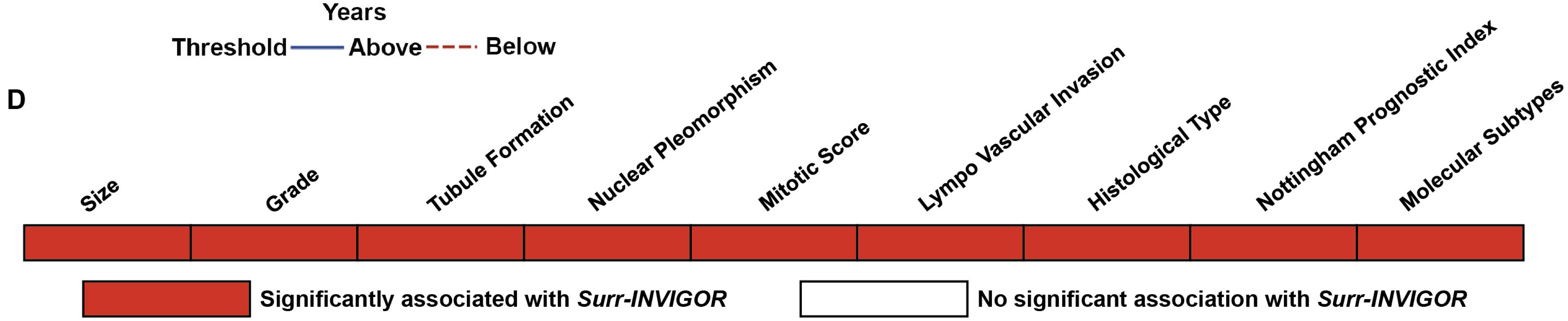

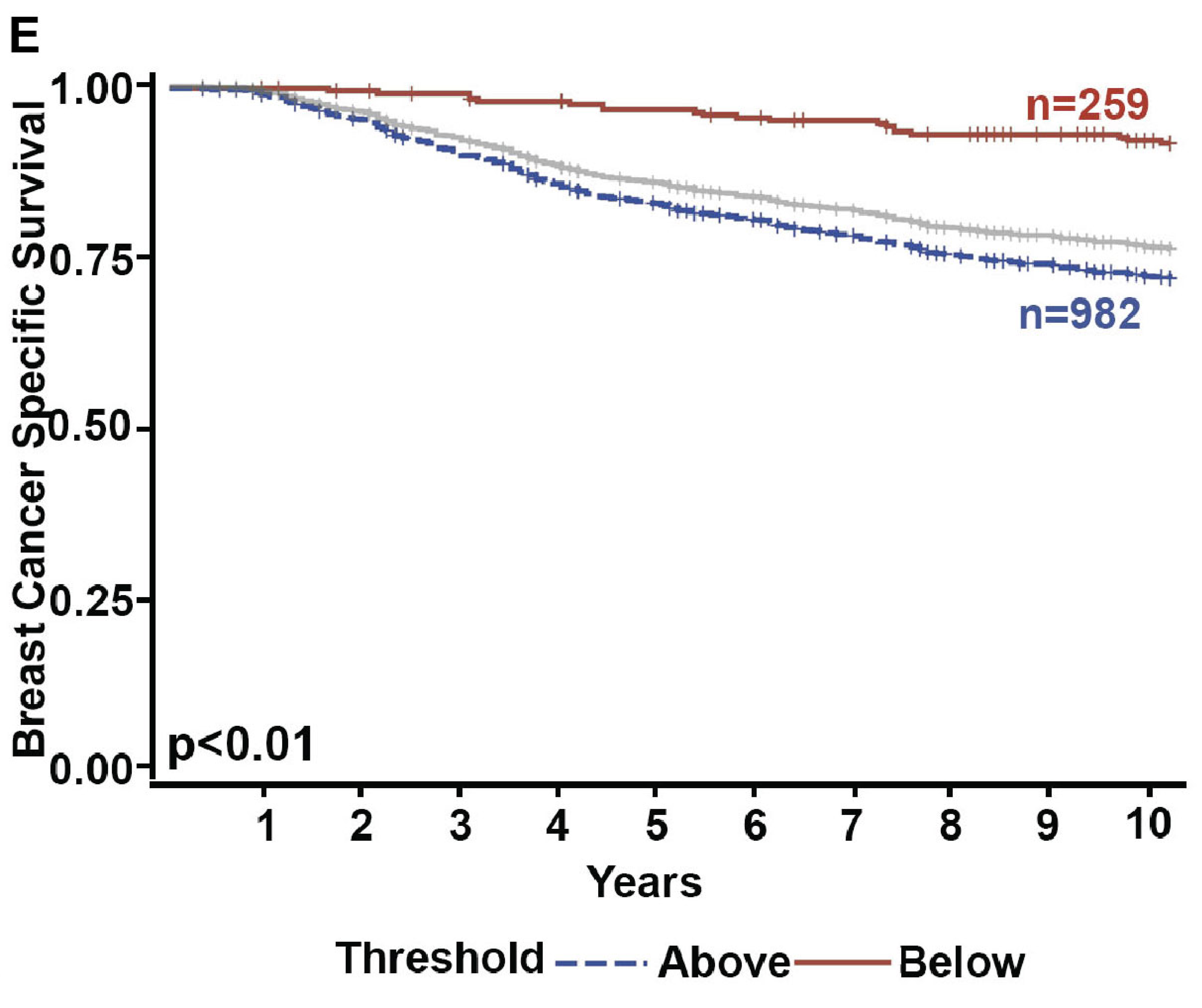

F

Multivariate analysis of the association between clinicopathological variables and patient's outcome in the validation cohort			
		Hazard Ratio (95% CI)	p-value
Overall Survival			
Age	≤65 vs >65	1.006 (0.994-1.018)	0.3242
ER	Neg	1.312 (1.008-1.707)	0.0435
Grade	3	7.204 (3.609-14.382)	<0.001
Grade	2	3.723 (1.853-7.481)	0.0002
Surr-INVIGOR	Above	2.059 (1.276-3.324)	0.0031

Table 1: Clinicopathological characteristics		
Parameters	**Study Cohort** **Number of cases (N; %)**	**Validation Cohort** **Number of cases (N; %)**
Age		
≤65	75 (81.5)	1057 (85.2)
>65	17 (18.5)	184 (14.8)
Tumor Grade		
1	16 (17.4)	325 (26.2)
2	42 (45.7)	501 (40.4)
3	34 (36.9)	415 (33.4)
Tumor Size		
≤15	32 (35.0)	969 (72.31)
>15	60 (65.0)	371 (27.69)
Lymph Node		
1	60 (65.2)	763 (61.5)
2	24 (26.1)	382 (30.8)
3	8 (8.7)	96 (7.7)
Hormone Receptor Status		
ER Positive	78 (84.8)	915 (73.7)
ER Negative	14 (15.2)	326 (26.3)
PR Positive	59 (64.1)	675 (54.4)
PR Negative	33 (35.9)	566 (45.6)
HER2 Expression		
Positive	5 (5.4)	151 (12.2)
Negative	81 (88.0)	1058 (85.3)
Missing	6 (6.5)	32 (2.6)
Intrinsic Molecular Subtypes		
Luminal A	38 (41.3)	408 (32.9)
Luminal B	28 (30.4)	429 (34.6)
HER2	5 (5.4)	151 (12.2)
BLBC	4 (4.3)	138 (11.1)
Triple Negative	11 (12.0)	68 (5.5)
Missing	6 (6.5)	47 (3.8)
Ki67		
High	44 (47.8)	667 (53.7)

Low	48 (52.2)	574 (46.3)
Tumor Type		
Invasive No Special Type	50 (54.3)	761 (61.3)
Invasive lobular	17 (18.5)	93 (7.5)
Tubular	11 (12.0)	299 (24.1)
Mucinous	2 (2.2)	11 (0.8)
Mixed type	12 (13.0)	77 (6.2)
Coexisting DCIS		
None	21 (23.0)	NA
Low grade	20 (22.0)	NA
Intermediate grade	22 (24.0)	NA
High grade	29 (31.0)	NA
Lympho-vascular Invasion		
Negative	60 (66.2)	686 (55.3)
Definite	21 (22.8)	397 (32.0)
Probable	11 (11)	158 (12.7)
Outcome Status		
Alive	62 (67.4)	650 (52.3)
Dead	30 (32.6)	591 (47.6)